

JGR Space Physics

RESEARCH ARTICLE

10.1029/2020JA028586

Key Points:

- During the first 25 periapses of the Juno mission, the Ultraviolet Spectrograph instrument observed transient bright spots at the edge of the swirl region
- During longer continuous observing sequences, the bright spots reoccurred at approximately the same System III location every ~25 min
- The bright spots were not fixed at noon or any other local time, which excludes any explanations involving an Earth-like noon-facing cusp

Supporting Information:

- Supporting Information S1
- Figure S1
- Figure S2
- Figure S3
- Figure S4

Correspondence to:

K. Haewsantati,
K.Haewsantati@uliege.be












Citation:

Haewsantati, K., Bonfond, B., Wannawichian, S., Gladstone, G. R., Hue, V., Versteeg, M. H., et al. (2021). Morphology of Jupiter's polar auroral bright spot emissions via Juno-UVS observations. *Journal of Geophysical Research: Space Physics*, 126, e2020JA028586. <https://doi.org/10.1029/2020JA028586>

Received 14 AUG 2020
 Accepted 28 JAN 2021

© 2021. American Geophysical Union.
 All Rights Reserved.

Morphology of Jupiter's Polar Auroral Bright Spot Emissions via Juno-UVS Observations

K. Haewsantati^{1,2,3} , B. Bonfond¹ , S. Wannawichian^{3,4} , G. R. Gladstone⁵ , V. Hue⁵ , M. H. Versteeg⁵ , T. K. Greathouse⁵, D. Grodent¹ , Z. Yao^{1,6} , W. Dunn^{7,8,9} , J.-C. Gérard¹ , R. Giles⁵, J. Kammer⁵, R. Guo¹, and M. F. Vogt¹⁰ 

¹LPAP, STAR Institute, Université de Liège, Liège, Belgium, ²Ph.D. Program in Physics, Department of Physics and Materials Science, Faculty of Science, Chiang Mai University, Chiang Mai, Thailand, ³National Astronomical Research Institute of Thailand (Public Organization), Chiang Mai, Thailand, ⁴Department of Physics and Materials Science, Faculty of Science, Chiang Mai University, Chiang Mai, Thailand, ⁵Southwest Research Institute, San Antonio, TX, USA, ⁶Key Laboratory of Earth and Planetary Physics, Institute of Geology and Geophysics, Chinese Academy of Sciences, Beijing, China, ⁷Mullard Space Science Laboratory, Department of Space and Climate Physics, University College London, Dorking, UK, ⁸The Centre for Planetary Science at UCL/Birkbeck, London, UK, ⁹Smithsonian Astrophysical Observatory, Harvard-Smithsonian Center for Astrophysics, Cambridge, MA, USA, ¹⁰Center for Space Physics, Boston University, Boston, MA, USA

Abstract Since 2016, the Juno-UVS (Ultraviolet Spectrograph) instrument has been taking spectral images of Jupiter's auroras in their full extent, including the nightside, which cannot be viewed from Earth. We present a systematic analysis of features in Jupiter's polar auroras called auroral bright spots, which were observed by Juno-UVS during the first 25 orbits of the spacecraft. An auroral bright spot is an isolated localized and transient brightening in the polar region. Bright spots were identified in 16 periapses (PJ) out of 24, mostly in either the northern or the southern hemisphere but rarely in both during the same PJ. The emitted power of the bright spots is time variable with peak power ranging from a few tens to a hundred of gigawatts. Moreover, we found that, for some PJs, bright spots exhibit quasiperiodic behavior. The spots, within PJ4 and PJ16, each reappeared within <2,000 km from the previous position in System III with periods of 28 and 22 min, respectively. This period is similar to periods previously identified in X-rays and various other observations. The bright spot positions are in a specific region in the northern hemisphere in System III, but are scattered around the magnetic pole in the southern hemisphere, near the edge of the swirl region. Furthermore, the bright spots can be seen at any local time, rather than being confined to the noon sector as previously thought from Earth-based observations. This suggests that the bright spots might not be firmly connected to the noon facing magnetospheric cusp processes.

1. Introduction

Jupiter's very bright ultraviolet (UV) auroras result from the collision between precipitating energetic particles and the atmospheric constituents in the planet's upper atmosphere. The auroras are generally divided into four components: The main emissions, the equatorward emissions, the polar emissions, and the satellites' footprints. The location, morphology and behavior of each component indicates that they are related to specific processes in different parts of the magnetosphere. The ever-present main emissions are the easiest feature to identify. They appear as a discontinuous contour around the magnetic pole. The northern hemisphere is subjected to a magnetic anomaly leading to regions of very strong and very weak magnetic field strength, which distorts the shape of the northern main emissions (Grodent et al., 2008). The main emissions are driven by internal processes in the middle magnetosphere at a radial distance of 20–60 Jovian radii (R_J) in the magnetosphere (Clarke et al., 2004; Vogt et al., 2011). The second component of Jupiter's aurora, the equatorward emissions, appear between the main emissions and Io's footpath and are mostly associated with magnetospheric injections (Dumont et al., 2014; Mauk et al., 2002). The multiple components of the satellite magnetic footprints are connected to the satellites of Jupiter via magnetic field lines (Bonfond, 2012). Lastly, polar auroras are characterized by the large variability of the auroral emissions in the entire region located poleward of the main emissions. The polar auroras are related to the dynamics of the outer magnetosphere, but the detailed mechanisms are still unclear. The UV polar emissions are divided into three subregions, the dark region, the swirl region, and the active region (Grodent et al., 2003). The

dark region is characterized by its crescent shape in the dawn sector within the main emission which appears dark in UV emission (Swithenbank-Harris et al., 2019). The swirl region is a region located around the magnetic pole which consists of numerous patchy and transient features whose motion is highly variable. Contrary to the behavior of the main emissions, where brightness and methane absorption are correlated (J. C. Gérard et al., 2016), the swirl region shows strong absorption signatures despite relatively dim emissions (Bonfond et al., 2017a). The active region, which lies poleward from the main emission in the noon to post-noon sector (Pallier & Prangé, 2001), is very dynamic. Flares, bright spots, and arc-like features are often observed in this region (Bonfond et al., 2016; Nichols et al., 2009; Waite et al., 2001).

One feature of the active region is the presence of “auroral bright spots” and these bright spots are the focus of this present study. Auroral bright spots have previously been studied by Pallier and Prangé (2001), who defined of the auroral bright spot as a transient emission located at the southern end of the transpolar brightening in the poleward direction from the main emissions. Their analysis made use of Hubble Space Telescope (HST) observations of Jupiter’s auroras, and they found that the locations of the bright spots typically varied in System III (hereafter SIII) longitude but were mostly located close to noon in magnetic local time (Pallier & Prangé, 2001, 2004). They therefore concluded that the bright spots could be linked to the Jovian cusp and either dayside or tail reconnection. However, the HST observations are limited in two ways. First, HST cannot explore the night side of the aurora and can only obtained limited views of the dawn and dusk sides. Second, the observations focused primarily on the northern aurora, as the southern emissions are closer to the pole and therefore more difficult to view from Earth. Since 2016, the Juno spacecraft has been in a polar orbit around Jupiter, providing unprecedented views of the planet’s auroral regions (Bolton et al., 2017). The ultraviolet spectrograph (UVS; Gladstone et al., 2017) can be used to produce images of Jupiter’s UV auroras covering all local times, providing the perfect opportunity to study the morphology of auroral bright spots in more detail than ever before.

Juno-UVS observations also provide the opportunity to study any periodicity in the auroral bright spot emission. Many types of quasiperiodic (QP) emission have been observed in Jupiter’s auroral region. The active regions also features polar flares, which were first reported by Waite et al. (2001) and were identified as short-lived but intense features in the active region that can suddenly brighten within a short time scale (10 s of seconds). Bonfond et al. (2011) found that southern polar flares reappear periodically with time intervals of 2–3 min, and Bonfond et al. (2016) revisited this study and found that these QP flares were present in half of their observing sequences. These features appeared in both northern and southern hemispheres, and some of them appeared to brighten in phase between the two hemispheres. From their location, size and behaviors, the flares appear to correspond to closed field lines mapping to the dayside outer magnetosphere. QP behavior has also been observed in the main emission region of the auroras; Nichols et al. (2017b) revealed a ~ 10 min period pulsating aurora feature in the main emission, which has the same period as the Alfvén wave travel time between the equatorial sheet and the ionosphere. Since so many features of the Jovian aurora display a quasiperiodic behavior, we investigate here whether the bright spot also brightens in a repetitive way.

Quasiperiodic pulsations have also been observed in many other datasets. McKibben et al. (1993) identified 40-minute periodicity in electron bursts observed by Ulysses, with a few cases showing shorter periods (2–3 min). Similarly, MacDowall et al. (1993) reported two classes of QP radio bursts with periods of 15 and 40 min, respectively. There was also a report by Pryor et al. (2005) of the correspondence of 2 min-long QP flares observed by Cassini Ultraviolet Imaging Spectrograph (UVIS) with low frequency radio bursts observed by Cassini Radio and Plasma Wave Spectrometer (RPWS) and Galileo Plasma Wave Spectrometer (PWS). Furthermore, many QP pulsations with periods in the range 10–100 min have been reported from the analysis of X-ray observations (Dunn et al., 2016, 2017, 2020; Elsner et al., 2005; Gladstone et al., 2002; Jackman et al., 2018; Weigt et al., 2020; Wibisono et al., 2020). Gladstone et al. (2002) presented the pulsation of emissions from a hot spot region in the northern hemisphere with period of 45 min. Elsner et al. (2005) showed the relation between X-ray pulsations with ~ 40 min period with Ulysses radio observation. Bunce et al. (2004) suggested that pulsed reconnection on the dayside magnetopause could be the source of the pulsations in both the X-ray and UV auroras.

So far, the only UV periodicities that have been observed in the active region of Jupiter’s polar auroras have had periodicities of 2–3 min, while QP emission in the X-ray and radio emission typically has a much longer

period (10 s of minutes). However, the maximum length for a continuous observation obtained from HST is about 45 min which limits the longest periodicity it can detect to about 20 min. HST observations cannot explore the night side of the aurora and are biased toward configurations in which the magnetic pole is tilted toward the Earth. In contrast, Juno-UVS allows for observations over a time period of up to 4 h, enabling us to search for variability on much longer timescales. In this study, we present a systematic study of the auroral bright spots observed by Juno-UVS during the first 25 orbits of the Juno mission. We discuss the observations and the bright spot detection method in Section 2, and we then discuss the results in Section 3. Juno provides an excellent view of Jupiter's polar regions at a range of local times, allowing us to study the locations of the bright spots in Section 3.1. Juno is also able to view the poles for an extended period of time during each orbit, allowing us to study the temporal variability of the bright spots in Section 3.2.

2. Juno-UVS Observations and Bright Spot Detection Methods

Juno is a spin-stabilized spacecraft that has been in a polar orbit around Jupiter since 2016. The Juno-UVS instrument is a UV photon-counting imaging spectrograph operating in the 68–210 nm wavelength range. There is a flat scan mirror at the entrance of the instrument, which allows it to look at targets up to $\pm 30^\circ$ away from the Juno spin plane. Its “dog bone” shaped slit consists of three contiguous segments with fields-of-view (FOV) of $0.2^\circ \times 2.5^\circ$, $0.025^\circ \times 2^\circ$, and $0.2^\circ \times 2.5^\circ$. The data obtained from UVS consist of a list of photon detection events with the X position of the photon count on the detector corresponding to the spectral dimension and the Y position corresponding to the spatial dimension along the slit (Gladstone et al., 2017; Greathouse et al., 2013; Hue et al., 2019). The spacecraft spins every ~ 30 s. Every spin, a spectrally resolved image can be reconstructed based on the motion of the field of view across the planet. The pointing mirror can target a different region of the aurora at each spin. Depending on the altitude of Jupiter, the area covered by the instrument during one Juno spin varies considerably; during the period of closest approach (PJ), a complete view of the auroras requires a combination of observations acquired during several consecutive spins. The polar projected images used for this study assume that the aurora originates from a mean altitude of 400 km above 1 bar level (Bonfond et al., 2015). For further analysis, the photon counts are converted to brightness in kilo-Rayleighs (kR) corresponding to the total unabsorbed H_2 Lyman emissions and Werner bands. The conversion is carried out by multiplying the intensity obtained in the 155–162 nm spectral range with a conversion factor of 8.1, based on the H_2 synthetic spectrum calculated by Gustin et al. (2013). The emitted power can then be computed by multiplying the brightness by the surface area and the mean energy of a UV photon. Uncertainty on the brightness calculation mainly comes from the in-flight calibration of the instrument effective area (Hue et al., 2019). In comparison, the uncertainty related to the shot noise is negligible here because we integrate over a relatively large region of the aurora (J. C. Gérard et al., 2019).

A bright spot is characterized as a distinct feature with a compact shape, which is very bright (typically more than 10 times brighter) in comparison to the surrounding area in the polar region. In order to identify the area of the bright spot, we first remove a mean background emission and then we consider regions with a brightness at least two times higher than the standard deviation of the brightness in the surrounding area. We then fit the shape of bright spot with an ellipse and we compute the emitted power in this ellipse. In this case, the main source of uncertainty lies in the selection of the area of interest. The uncertainty is therefore calculated by assuming an elliptical reference area 25% smaller and then 25% larger than the best fit ellipse. To assess the evolution of the total power in the region of interest, the ellipse area is fitted based only on the images for which the bright spot can be clearly identified. Then, for a given data set (i.e., a specific spot during a given perijove), the union of the fitted ellipses is used as a reference surface to compute the total power, so that the area of interest remains the same during the whole sequence.

3. Results

From UVS data obtained during the first 25 perijoves (PJ), bright spots appear in both northern and southern hemispheres. An example from each hemisphere is shown in Figure 1. Northern hemisphere bright spots have been identified during 5 perijoves (PJ1, PJ3, PJ6, PJ8, and PJ13) and southern hemisphere bright spots have been identified during 12 perijoves (PJ4, PJ8, PJ9, PJ12, PJ14, PJ15, PJ16, PJ20, PJ21, PJ22, PJ23, and PJ24). It should be noted that PJ3, PJ12, PJ21,

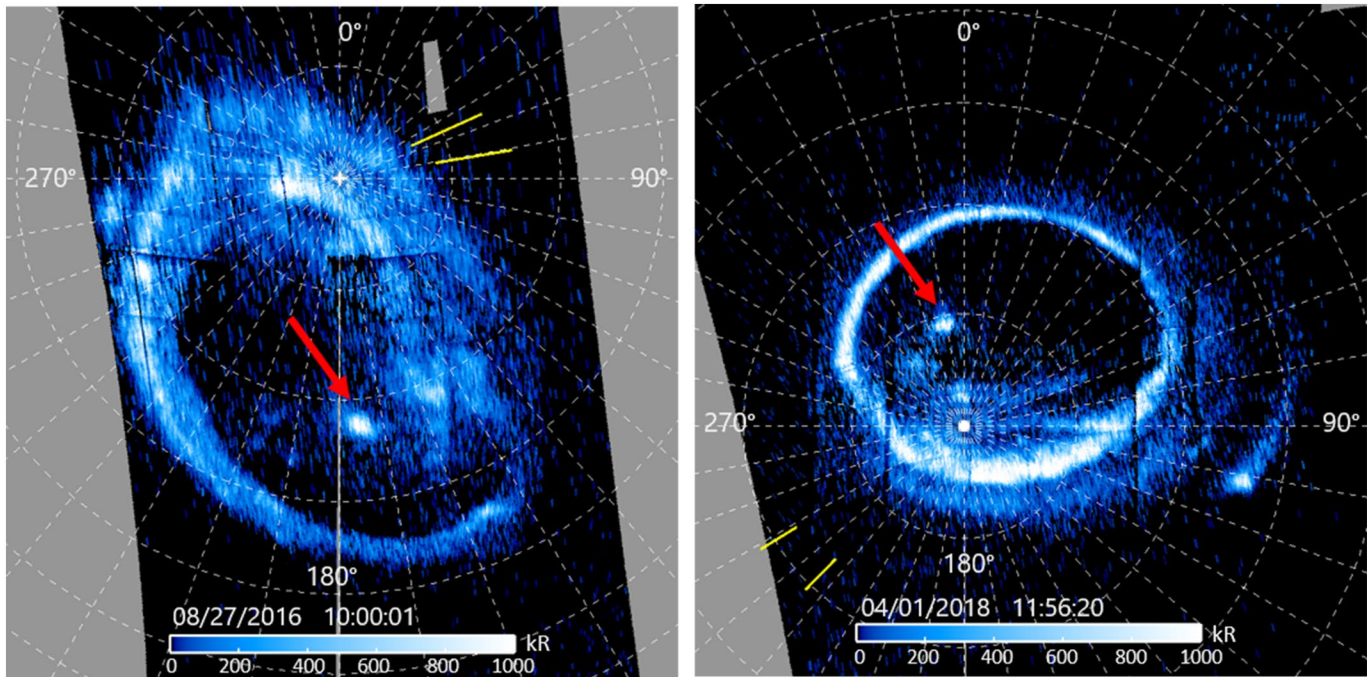


Figure 1. Two examples of bright spots in Jupiter's polar auroras (indicated by red arrows) as observed by Juno-UVS in the northern hemisphere during PJ11 (left) and the southern hemisphere during PJ12 (right). The grid represents meridians and parallels in the SIII, spaced every 10°. Each polar projection is a combination of observations acquired during several spins in order to create a full view of Jupiter's aurora. The two short, yellow lines in each frame show the subsolar longitudes at the start time and stop time of combined data. PJ, perijoves; UVS, Ultraviolet Spectrograph.

and PJ23 each contain bright spots at two distinct positions. The bright spots sometimes appear as compact small spots, with smallest surface area $3.5 \times 10^5 \text{ km}^2$, and sometimes it covers a larger area ($2.07 \times 10^7 \text{ km}^2$). The total power emission usually lies in the range of tens of gigawatts (GW), but some spots' power can occasionally rise up to a hundred GW (e.g., PJ16 at 01:52:04, cf. Figure 7). The summary of bright spots area, power, magnetic flux corresponding to the spot's area, and the local time in Jupiter's ionosphere are shown in Figure 2. In the next subsections, we will discuss the variability of the bright spots' power and position. We find that the bright spots usually reappear at nearly the same position in SIII coordinates, that is within a few degrees from their first detected position. Moreover, the time intervals between the occurrence of consecutive spots in a given perijove range from a few minutes to more than half an hour.

3.1. Location and Local Time

3.1.1. Position in System III

The pixel positions of the peak of bright spots were used to calculate the latitudinal and longitudinal coordinates of spot features in the ionosphere. The bright spots in the northern hemisphere are mostly clustered in a restricted region. As shown in Figure 3, the positions of the bright spots, except for PJ8 data (marked as a green cross), are located within 60–70°N planetocentric latitude and 160–190°W (SIII). Incidentally, this region is also the X-ray hot spot region (Dunn et al., 2016, 2017, 2020; Gladstone et al., 2002; Weigt et al., 2020). One notable exception is found during PJ8, where the bright spot is located at $\sim 82^\circ\text{N}$ and 216.5°W (SIII). In contrast, the bright spots detected in the southern hemisphere scatter around the magnetic pole.

In addition to showing the SIII positions of the bright spots, Figure 3 also shows the surface magnetic field strength from the Joint Replacement Models (JRM09) model (Connerney et al., 2018). Considering the two hemispheres together, it appears that the bright spots favor areas where the surface magnetic field strength is larger than $8 \times 10^5 \text{ nT}$. Once again, the exception is the bright spot observed in the north during PJ8, which was one of the dimmest bright spots observed. Greathouse et al. (2017) noted that the brightness of swirl region depends on the orientation of the magnetic dipole relative to the sun. In particular, they found

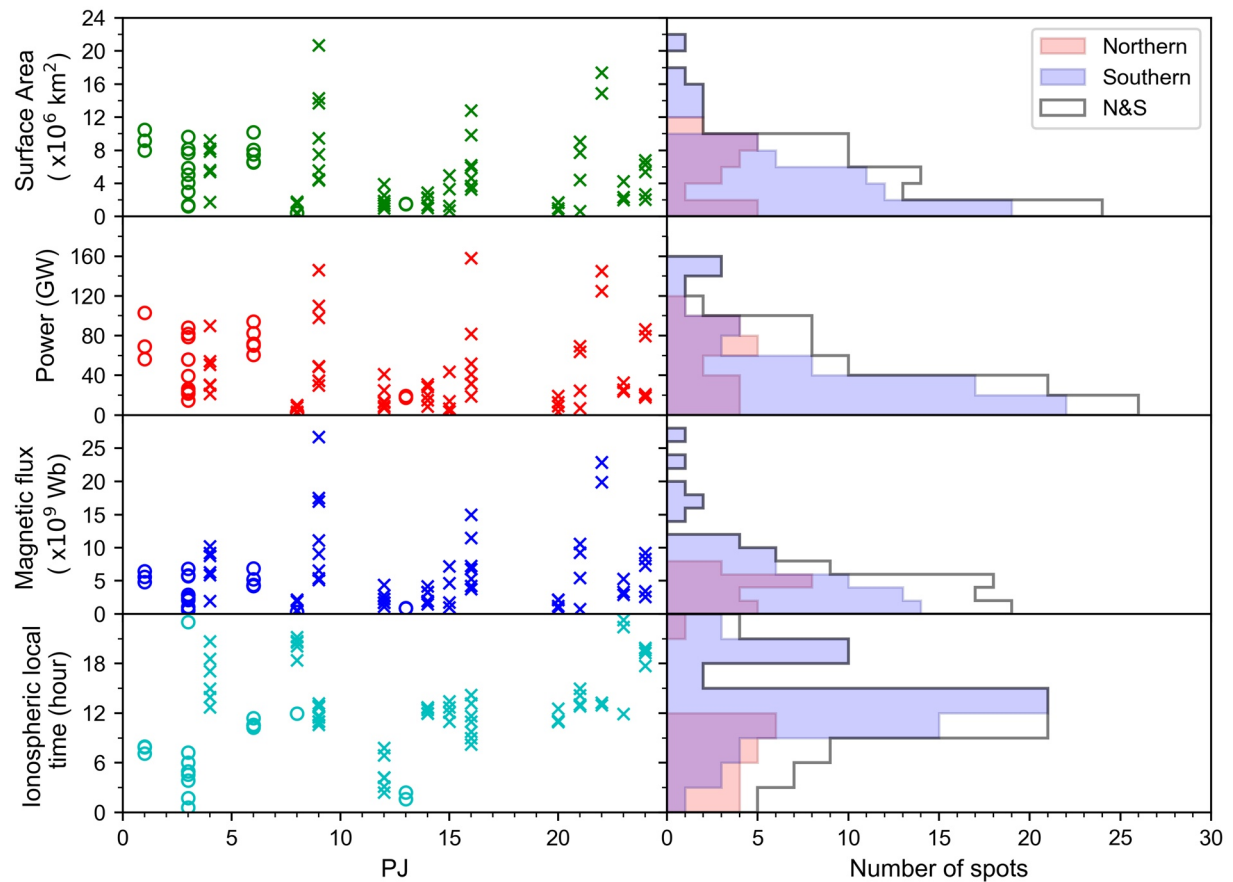


Figure 2. A summary of the properties of the auroral bright spots observed by Juno-UVS. The top three panels show distribution of the surface area, the power emission, and the magnetic flux inside bright spot's area based on elliptical fit. The bottom panel shows the ionospheric local time at the bright spot's peak emission. On the left panels, those values vary at different PJs, for the northern spots (circles) and the southern spots (crosses). The right panels combine the data from all perijoves into histograms. PJ, perijoves; UVS, Ultraviolet Spectrograph.

that the swirl region is brighter when it faces the sun. On the other hand, the solar illumination does not seem to play a major role in the ionospheric conductivity, which is one of the possible parameters controlling the auroral brightness. From radar observations, Galand and Richmond (2001) concluded that the solar UV flux does not contribute significantly to the ionization of the upper atmosphere neutrals, contrary to the precipitation of electrons and ions (e.g., Ballester et al., 2018; J. C. Gérard et al., 2020). We therefore investigated whether the bright spot behaves in the same way as the swirl region. To do so, we calculated the solar zenith angle at the bright spot position, as shown in Figure 4, and we found that the bright spot occurs even when the sun is at high zenith angle or even below the horizon.

3.1.2. Position With Respect to the Swirl Region

In order to study the location of the bright spots with respect to the swirl region, we plotted the bright spot locations on top of color ratio maps for each perijove. The color ratio is defined as the ratio between emission intensity of molecular hydrogen at two wavelength ranges, one unaffected by methane absorption (1,550–1,620 Å) and one affected by methane absorption (1,250–1,300 Å). On these maps, the swirl region displays distinctive strong absorption signatures (Bonfond et al., 2017a). Figure 5 shows examples of such color ratio maps from PJ6 (north, left) and PJ16 (south, right) with the position of the bright spots identified during these perijoves overplotted. By looking at all perijoves, we find that that the brightest spots are located near the boundary of the high color ratio regions (swirl region). The biggest outlier was PJ1, for which the bright spots are located inside the high color ratio region instead of at its boundary (see Figure S2).

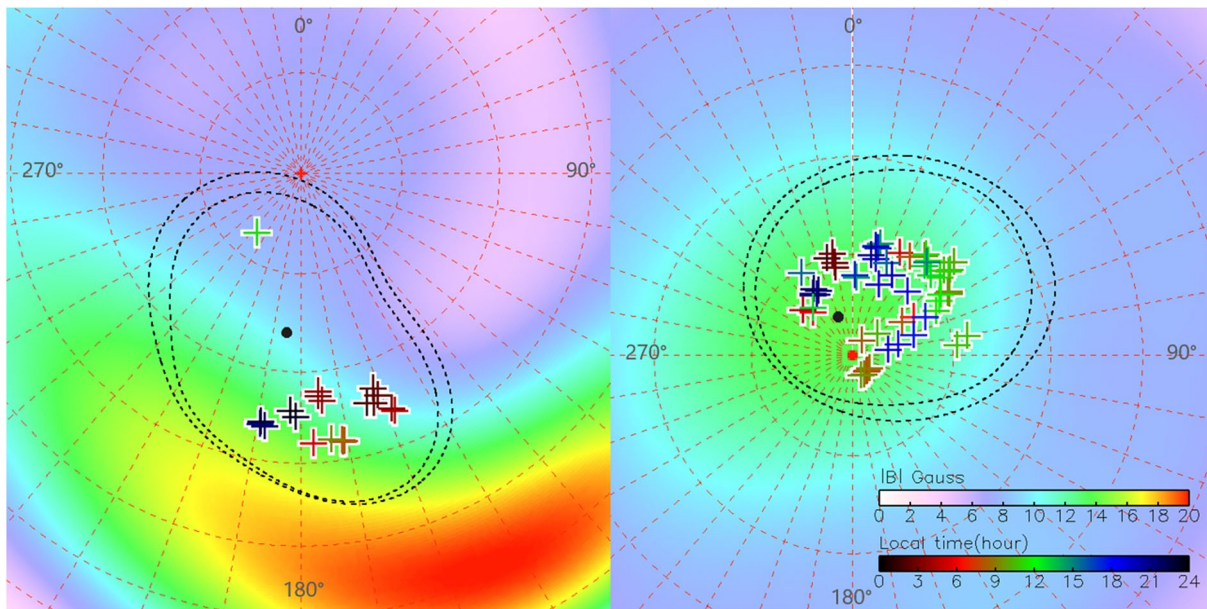


Figure 3. Polar projections with the same coordinates as Figure 1, show the magnetic field magnitude (in Gauss) on the surface of Jupiter based on JRM09 model (Connerney et al., 2018) and the positions of bright spots observed in Jupiter's polar region for (left) northern and (right) southern hemispheres. The two dashed contours are the statistical locations of the main emission for the compressed (inner contour) and expanded (outer contour) cases observed by HST in 2007 (Bonfond et al., 2012). The black dot indicates the magnetic pole of each hemisphere (Bonfond et al., 2017b; Connerney et al., 2018). The colors of the bright spot markers correspond to their magnetic local times, calculated from the magnetic mapping model developed by Vogt et al. (2011, 2015) coupled with the JRM09 model. HST, Hubble Space Telescope; JRM, Joint Replacement Models.

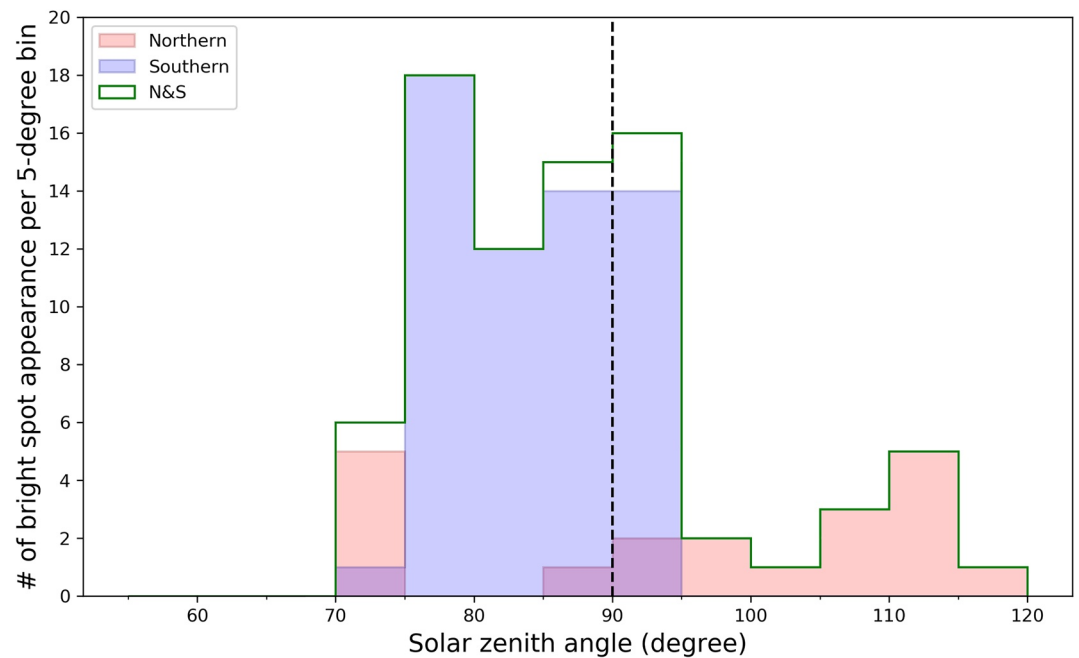


Figure 4. Distribution of solar zenith angles of bright spots in the northern hemisphere (pink), Southern hemisphere (blue), and the combined spots from both hemispheres (green line). The dashed vertical line represents 90° solar zenith angle at which the sun is on the horizon. The angles larger than 90° refer to case when the sun is below the horizon, corresponding to the night time.

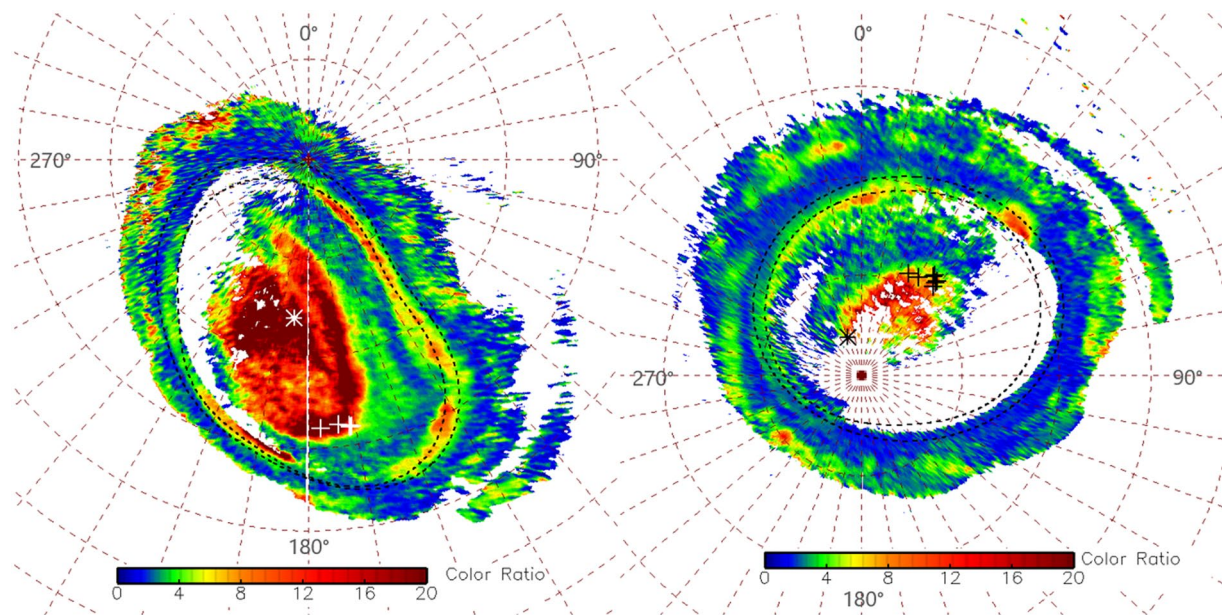


Figure 5. The bright spots positions and the color ratio map observed from (left) PJ6 and (right) PJ16. The coordinates and two dashed contours are described in Figure 1. The plus signs are the bright spots observed in (left) PJ6 and (right) PJ16. The asterisk signs represent the magnetic poles, for (left) north and (right) south hemispheres (Bonfond et al., 2017b; Connerney et al., 2018). PJ, perijoves.

3.1.3. Position in Magnetic Local Time

Observations carried out with HST suggested that the auroral bright spots are primarily located in the magnetic noon sector (Pallier & Prangé, 2001). However, HST observations are biased in favor of configurations for which the magnetic pole faces the Earth and the night side of the aurora is out of sight. On the contrary, Juno-UVS provides complete views of the aurora, including the nightside, whatever the orientation of the dipole. In this section, the local time of the bright spot in the magnetosphere is studied by using the magnetic mapping model. Inferring the magnetic local time of polar auroral features becomes increasingly uncertain poleward of the satellite footprints' reference ovals. However, this uncertainty will not prevent any estimate of the magnetic local time, because the exact number of the local time is not the main interest, but instead we are interested in the broad sector to which the aurora connect. One of the most important characteristics required from the magnetic field model is the capability to account for the bendback of the magnetic field lines and to accurately represent the topology of the field close to the planet. Therefore, we chose the publicly available magnetosphere-ionosphere mapping flux equivalence method of Vogt et al. (2011, 2015) coupled with the JRM09 internal magnetic field model (Connerney et al., 2018) to evaluate the magnetospheric source location and local time in the outer magnetosphere.

The mapping results show that the bright spots are generally mapping to positions beyond $150 R_J$ or beyond the dayside magnetopause, which means the positions are beyond the model's limit. In order to estimate the result despite these limitations, we extrapolate the spots' position radially until we obtain a predicted position from the model. This can be done by tracing a line on the polar plot, from the magnetic pole toward the bright spot's position and keep moving equatorward until we obtain the latitude and longitude that can be mapped to a position inside the model boundary. In the southern hemisphere, we chose the point where the JRM09 magnetic field is vertical as the southern magnetic pole, at approximately -86°N and 340°W (SIII). In the northern hemisphere, the magnetic field is so complex that there is no point where the field is vertical in the auroral polar region. Hence, we chose the barycenter of the aurora as defined in Bonfond et al. (2017b), at 74°N and 185°W (SIII). The polar projection maps of bright spots and the corresponding magnetic local time are shown by the color of the crosses in Figure 3. The local times of the bright spots in the northern hemisphere range from late evening through midnight to late morning while the local times for bright spot in the southern hemisphere spread in entire range. As well as calculating the magnetic local time of each spot, we also calculated the ionospheric local time, which takes the magnetic pole defined

above as the center and the Sun direction as noon. The ionospheric local times are shown in Figure 2, and their distribution is similar to the distribution of magnetic local times. These local times surprised us that this feature can appear on the night time as well. This wide distribution of local times significantly contrasts with previous studies (Pallier & Prangé, 2001, 2004) which suggested that the bright spot could correspond to noon local time facing magnetospheric cusp. This discrepancy is likely to be due to the fact that the previous studies were essentially based on images of Jupiter with the magnetic pole oriented toward HST and restricted to the dayside of Jupiter. Therefore, because of these biases, their results focus on local times compatible with a connection to the magnetospheric cusp.

3.1.4. Bright Spot's Motion With Time

Figure 6 shows the locations of the observed bright spots on a cylindrical map. In most perijoves with bright spots, they were observed on multiple occasions, and Figure 6 shows how their locations vary with time. Please note that this figure shows both the bright spots in the same plot which are separated by different colors. In most cases, the positions of the northern and southern spots only change slightly in both latitude and longitude (a few thousand kilometers). The only spots whose locations vary noticeably are the northern spot from PJ3 and the southern spots from PJ9, PJ16 and PJ24. The motions of the bright spots at latitudes beyond $\pm 85^\circ$, that is, PJ14 and PJ15, are actually very small because the positions lie close to the rotational pole. The bright spot found in PJ3 in the north (deep blue symbol in Figure 6), shows the variation in position starting from 164°W to 158°W in longitude and 3° shifted in latitude. For the bright spot in the southern hemisphere, the bright spot from PJ9 appears to move from low to high latitude starting from -76°N to -80°N and from 47°W to 62°W in longitude while a bright spot from PJ24 continuously change position from 20°W to 70°W in longitude. These results show that the bright spots are mostly fixed in specific positions as Jupiter rotates, while, in a few cases, their positions changed. The rates of change in positions are also not related to Jupiter's rotation period. Moreover, the motions do not have any systematic pattern since we found cases where the SIII longitude increased or decreased over time.

3.2. The Bright Spot's Power Variations

Polar emissions have previously been observed to be quasiperiodic with periods varying from a few minutes to several tens of minutes. In this section, we investigate whether the auroral bright spots are also a form of QP emission. Since Section 3.1.4 showed that the bright spots reappear at nearly the same position, we consider the emissions in the same region to be part of a continuous sequence. In many cases, we can see the bright spot brighten and fade with a time interval on the order of minutes. When we consider the whole available data set, this time interval is in the 3–47 min range.

The continuous tracking of the bright spot emitted power is complicated by the fact that the field-of-view of the instrument varies significantly with time, which leads to discontinuous sampling rate, or inappropriately short sequences, to investigate periodicities over many cycles. Moreover, as the mission progressed, the duration of the observations in the northern hemisphere decreased from a few hours to a few tens of minutes. Fortunately, two particular cases, from PJ4 and PJ16 in the South, allowed for a quasicontinuous monitoring of the bright spots' power variations for 3–4 h.

Figure 7 shows the power variation as a function of time for one particular southern bright spot during PJ16 (a similar plot for PJ4 can be found in the supplemental material). The shaded areas indicate time intervals during which UVS field-of-view missed more than 50% of the region of interest defined by the union of the fitted ellipses. The power peaks of the bright spot are above 35 GW and can reach up to 170 GW. Moreover, a clear repetitive pattern is identified in the time series, that is, the power reaches a peak every ~ 30 min. In addition to the well-identified bright spots (black arrows), the plot shows that there are additional power peaks (indicated by red arrows) that correspond to more diffuse features that were not identified as bright spots at first. Nevertheless, these power peaks are close to shaded areas, suggesting that UVS might have missed the time interval during which a clear bright spot could have been identified. The time intervals between consecutive peaks in this plot ranges from 5 to 40 min, with a typical interval around 25 min. In order to get quantitative results, we also determine the spot's reappearance period with a Lomb-Scargle analysis, which is suitable for analyzing discontinuous time series data (see Figure S4). The results confirm that the bright spot emissions PJ16 repeatedly brighten with period of 23 min. Results from PJ4 shows a similar

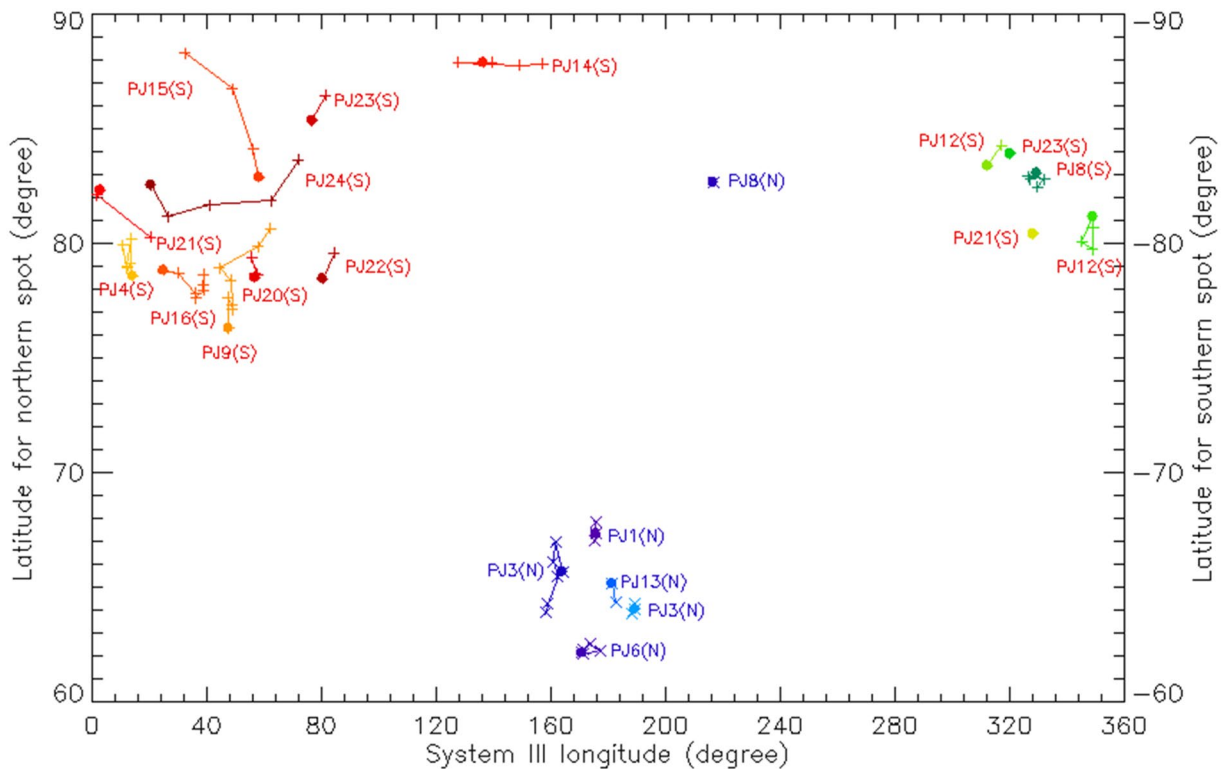


Figure 6. Latitude and SIII longitude map shows the positions of bright spot observed in northern hemisphere (plus sign) and southern hemisphere (cross sign). Each line is named by the perijove number and the hemisphere, for example, PJ1(N) is for northern bright spot from PJ1. The northern spots are colored in shades of blue and southern spots use a color gradient from green to red. The line connecting each data presents the motion of bright spot with observing time order. The large dot for each line represents the first position of the bright spot during a sequence. PJ, perijoves.

pattern with a ~ 28 min period. The periodicity of these auroral bright spots is considerably longer than the 2–3-minute periods of the polar flares (Bonfond et al., 2011, 2016), which also occur in a similar part of the aurora. These 20–30-min periods are however similar to other reports of quasiperiodic phenomena in Jupiter's polar regions (Dunn et al., 2016; Jackman et al., 2018; MacDowall et al., 1993; McKibben et al., 1993; Wibisono et al., 2020).

4. Discussions and Conclusions

Based on the previous observations of Pallier and Prangé (2001), we expected that the bright spots would appear near noon magnetic local time corresponding to the Jovian magnetospheric cusp. Instead, our results show that the bright spots can be seen in various ionospheric local times and are observed at positions mapping to a wide range of magnetic local times in the distant magnetosphere. Moreover, several bright spots were observed at different locations during the same observational sequence. We show that the bright spots mostly lie near the edge of the swirl region (with one exception during PJ1). Furthermore, we show that in 18 cases out of 20, bright spots reappear at approximately the same SIII position during a given sequence, suggesting that the source region (wherever it is along the field line) corotates with Jupiter. Moreover, the local time results thus rule out the possibility that the bright spot is direct counterpart of a noon-facing magnetospheric cusp, under the assumption that the magnetospheric topology in the polar region is simple. On the other hand, Zhang et al. (2020) suggested that topology of the polar-most field lines could be very complex and helical, leading to atypical definition of a magnetospheric cusp for Jupiter and an unclear mapping of the field lines. If this model actually reflects the complexity and entanglement of the high latitude field lines, then we cannot exclude that the bright spots could be related to some cusp-like processes, but these would be much more complex than expected from an analogy with the Earth.

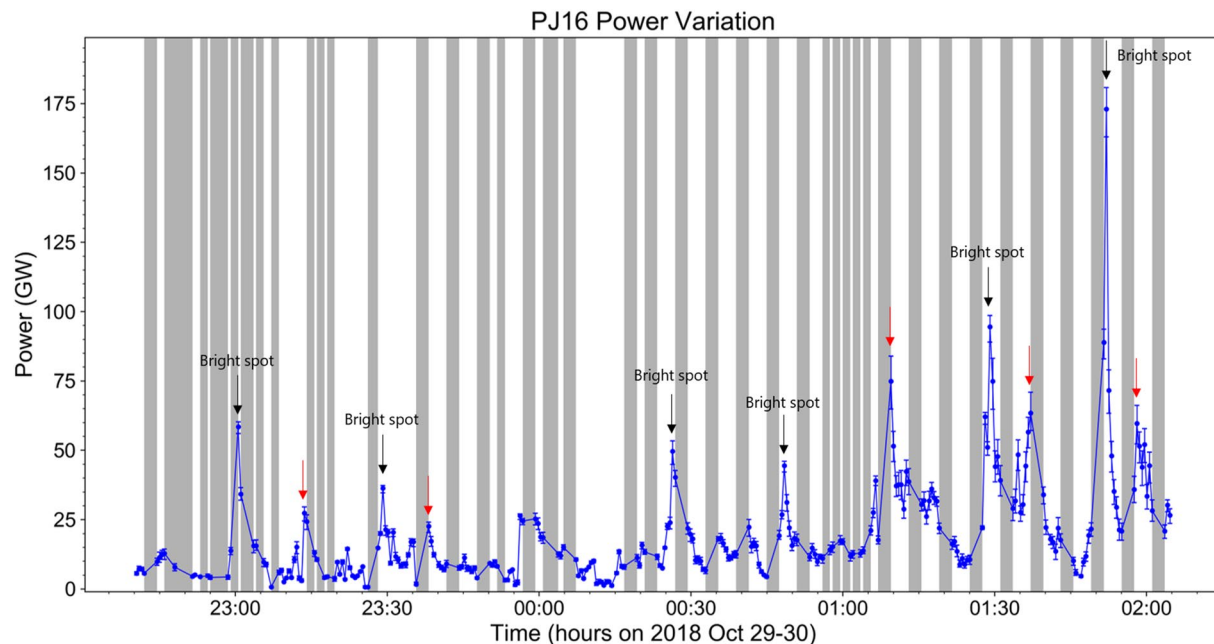


Figure 7. The time variation of power emission observed in PJ16 from 22:40:00 UT on October 29, 2018 to 02:00:00 UT on October 30, 2018. The gray boxes illustrate the times that >50% of the bright spot region was not covered by the UVS field-of-view. Black arrows indicate the times when clear bright spots are detected while red arrows show the additional peaks at which no bright spot appears in the region of interest. The error bars correspond to the 25% range of ellipse area, at which the integrated power is nearly constant. UVS, Ultraviolet Spectrograph.

Acknowledgments

K. Haewsantati would like to grateful thank for financial support from Science Achievement Scholarship of Thailand (SAST) and Ph.D. program in Physics, Chiang Mai university. K. Haewsantati and S. Wannawichian, are supported by National Astronomical Research Institute of Thailand (NARIT). B. Bonfond is a Research Associate of the Fonds de la Recherche Scientifique - FNRS. B. Bonfond, D. Grodent, Z. Yao and J. C. Gerard acknowledge the support from the PRODEX Program of European Space Agency (ESA). G. R. Gladstone, V. Hue, M. H. Versteeg, and T. K. Greathouse, are funded by the Southwest Research Institute. W. Dunn is supported by STFC research grant to UCL and SAO fellowship to Harvard-Smithsonian Centre for Astrophysics and by ESA. R. Giles is supported by the Incoming PostDocs in Sciences, Technology, Engineering, Materials and Agrobiotechnology (IPD-STEMA) project from Université de Liège. This research was partly supported by NARIT. Additional support was from Thailand Science Research and Innovation grant RTA6280002. We are grateful to NASA and contributing institutions which have made the Juno mission possible. This work was funded by NASA's New Frontiers Program for Juno via contract with the Southwest Research Institute.

Finally, our study of the variations of the emitted power shows that the bright spots are not sporadic random events, since they reoccur multiple times at nearly the same position. The bright spot emissions observed during PJ4 and PJ16 are particularly interesting because of the length of the observed sequence, and quasiperiodicities of 22–28 min are detected. Such timescales are hard to identify with the limited duration of HST observations (~45 min). Even if we do not exclude a possible relationship between the bright spots and the flares, it should be noted that the periodicities identified here for the bright spots are one order of magnitude longer (~30 min) than the one identified for the 2–3 min QP flares (Bonfond et al., 2011; Bonfond et al., 2016; Nichols et al., 2017a). Moreover, while most of the bright spots appear close to the boundary of the swirl region, the flares instead take place on the noon and dusk sides of the active region (Bonfond et al., 2016; Nichols et al., 2017a). Instead, the reappearances of bright spots several times during the same day suggest a link with other quasiperiodic behavior with similar time scales. It should be noted that the 3–47 min time intervals between consecutive emissions are also the same range as quasiperiodic pulsations identified in radio emissions (MacDowall et al., 1993), relativistic electrons (McKibben et al., 1993), Alfvén waves (Manners et al., 2018) and X-ray pulsations (Jackman et al., 2018; Wibisono et al., 2020). Further studies of the connection between these different phenomena will certainly provide important information concerning the processes giving rise to these emissions.

Data Availability Statement

The data included herein are archived in NASA's Planetary Data System (https://pds-atmospheres.nmsu.edu/data_and_services/atmospheres_data/JUNO/uv.html).

References

- Ballester, J. L., Alexeev, I., Collados, M., Downes, T., Pfaff, R. F., Gilbert, H., et al. (2018). Partially ionized plasmas in astrophysics. *Space Science Reviews*, 214(2), 58. <https://doi.org/10.1007/s11214-018-0485-6>
- Bolton, S. J., Lunine, J., Stevenson, D., Connerney, J. E. P., Levin, S., Owen, T. C., et al. (2017). The Juno mission. *Space Science Reviews*, 213(1–4), 5–37. <https://doi.org/10.1007/s11214-017-0429-6>
- Bonfond, B. (2012). When Moons Create Aurora: The Satellite Footprints on Giant Planets. In A. Keiling, E. Donovan, F. Bagenal, & T. Karlsson (Eds.), *Auroral Phenomenology and Magnetospheric Processes*. <https://doi.org/10.1029/2011GM001169>

- Bonfond, B., Gladstone, G. R., Grodent, D., Greathouse, T. K., Versteeg, M. H., Hue, V., et al. (2017a). Morphology of the UV aurorae Jupiter during Juno's first perijove observations. *Geophysical Research Letters*, *44*(10), 4463–4471. <https://doi.org/10.1002/2017GL073114>
- Bonfond, B., Grodent, D., Badman, S. V., Gérard, J.-C., & Radioti, A. (2016). Dynamics of the flares in the active polar region of Jupiter. *Geophysical Research Letters*, *43*(23), 11963–11970. <https://doi.org/10.1002/2016GL071757>
- Bonfond, B., Grodent, D., Gérard, J.-C., Stallard, T., Clarke, J. T., Yoneda, M., et al. (2012). Auroral evidence of Io's control over the magnetosphere of Jupiter. *Geophysical Research Letters*, *39*(1), L01105. <https://doi.org/10.1029/2011GL050253>
- Bonfond, B., Gustin, J., Gérard, J.-C., Grodent, D., Radioti, A., Palmaerts, B., et al. (2015). The far-ultraviolet main auroral emission at Jupiter – Part 2: Vertical emission profile. *Annales Geophysicae*, *33*(10), 1211–1219. <https://doi.org/10.5194/angeo-33-1211-2015>
- Bonfond, B., Saur, J., Grodent, D., Badman, S. V., Bisikalo, D., Shematovich, V., et al. (2017b). The tails of the satellite auroral footprints at Jupiter. *Journal of Geophysical Research: Space Physics*, *122*(8), 7985–7996. <https://doi.org/10.1002/2017JA024370>
- Bonfond, B., Vogt, M. F., Gérard, J.-C., Grodent, D., Radioti, A., & Coumans, V. (2011). Quasi-periodic polar flares at Jupiter: A signature of pulsed dayside reconnections? *Geophysical Research Letters*, *38*(2), L02104. <https://doi.org/10.1029/2010GL045981>
- Bunce, E. J., Cowley, S. W. H., & Yeoman, T. K. (2004). Jovian cusp processes: Implications for the polar aurora. *Journal of Geophysical Research*, *109*(A9), A09S13. <https://doi.org/10.1029/2003JA010280>
- Clarke, J. T., Grodent, D., Cowley, S. W. H., Bunce, E. J., Zarka, P., Connerney, J. E. P., et al. (2004). Jupiter's aurora. In F. Bagenal, T. Dowling, & W. McKinnon (Eds.), *Jupiter: The Planet, Satellites and Magnetosphere*. Cambridge University Press (pp. 639–670).
- Connerney, J. E. P., Kotsiaros, S., Oliverson, R. J., Espley, J. R., Joergensen, P. S., et al. (2018). A new model of Jupiter's magnetic field from Juno's first nine orbits. *Geophysical Research Letters*, *45*(6), 2590–2596. <https://doi.org/10.1002/2018GL077312>
- Dumont, M., Grodent, D., Radioti, A., Bonfond, B., & Gérard, J.-C. (2014). Jupiter's equatorward auroral features: Possible signatures of magnetospheric injections. *Journal of Geophysical Research: Space Physics*, *119*(12), 10068–10077. <https://doi.org/10.1002/2014JA020527>
- Dunn, W. R., Branduardi-Raymont, G., Elsner, R. F., Vogt, M. F., Lamy, L., Ford, P. G., et al. (2016). The impact of an ICME on the Jovian X-ray aurora. *Journal of Geophysical Research: Space Physics*, *121*(3), 2274–2307. <https://doi.org/10.1002/2015JA021888>
- Dunn, W. R., Branduardi-Raymont, G., Ray, L. C., Jackman, C. M., Kraft, R. P., Elsner, R. F., et al. (2017). The independent pulsations of Jupiter's northern and southern X-ray auroras. *Nature Astronomy*, *1*(11), 758–764. <https://doi.org/10.1038/s41550-017-0262-6>
- Dunn, W. R., Gray, R., Wibisono, A. D., Lamy, L., Louis, C., Badman, S. V., et al. (2020). Comparisons Between Jupiter's X-ray, UV and Radio Emissions and In Situ Solar Wind Measurements During 2007. *Journal of Geophysical Research: Space Physics*, *125*(6), e2019JA027222. <https://doi.org/10.1029/2019JA027222>
- Elsner, R. F., Lugaz, N., Waite, J. H., Cravens, T. E., Gladstone, G. R., Ford, P., et al. (2005). Simultaneous Chandra X ray, Hubble Space Telescope ultraviolet, and Ulysses radio observations of Jupiter's aurora. *Journal of Geophysical Research*, *110*(A1), A01207. <https://doi.org/10.1029/2004JA010717>
- Galand, M., & Richmond, A. D. (2001). Ionospheric electrical conductances produced by auroral proton precipitation. *Journal of Geophysical Research: Space Physics*, *106*, 117–125. <https://doi.org/10.1029/1999JA002001>
- Gérard, J.-C., Bonfond, B., Grodent, D., & Radioti, A. (2016). The color ratio-intensity relation in the Jovian aurora: Hubble observations of auroral components. *Planetary and Space Science*, *131*, 14–23. <https://doi.org/10.1016/j.pss.2016.06.004>
- Gérard, J.-C., Bonfond, B., Mauk, B. H., Gladstone, G. R., Yao, Z. H., Greathouse, T. K., et al. (2019). Contemporaneous Observations of Jovian Energetic Auroral Electrons and Ultraviolet Emissions by the Juno Spacecraft. *Journal of Geophysical Research: Space Physics*, *124*(11), 8298–8317. <https://doi.org/10.1029/2019JA026862>
- Gérard, J.-C., Gkouvelis, L., Bonfond, B., Grodent, D., Gladstone, G. R., Hue, V., et al. (2020). Spatial distribution of the pedersen conductance in the jovian aurora from Juno-UVS spectral images. *Journal of Geophysical Research: Space Physics*, *125*(8), e2020JA028142. <https://doi.org/10.1029/2020JA028142>
- Gladstone, G. R., Jr, J. H. W., Grodent, D., Lewis, W. S., Crary, F. J., Elsner, R. F., et al. (2002). A pulsating auroral X-ray hot spot on Jupiter. *Nature*, *415*(6875), 1000–1003. <https://doi.org/10.1038/4151000a>
- Gladstone, G. R., Persyn, S. C., Eterno, J. S., Walther, B. C., Slater, D. C., Davis, M. W., et al. (2017). The Ultraviolet Spectrograph on NASA's Juno Mission. *Space Science Reviews*, *213*(1), 447–473. <https://doi.org/10.1007/s11214-014-0040-z>
- Greathouse, T. K., Gladstone, G. R., Davis, M. W., Slater, D. C., Versteeg, M. H., Persson, K. B., et al. (2013). Performance results from in-flight commissioning of the Juno Ultraviolet Spectrograph (Juno-UVS). In *UV, X-ray, and gamma-ray Space instrumentation for astronomy XVIII*. International Society for Optics and Photonics, Vol. 8859, (p. 88590T). <https://doi.org/10.1117/12.2024537>
- Greathouse, T. K., Gladstone, G. R., Versteeg, M. H., Hue, V., Kammer, J., Davis, M. W., et al. (2017). A Study of Local Time Variations of Jupiter's Ultraviolet Aurora using Juno-UVS. In *AGU fall meeting abstracts*. Vol. 2017 (pp. P24A–07).
- Grodent, D., Bonfond, B., Gérard, J.-C., Radioti, A., Gustin, J., Clarke, J. T., et al. (2008). Auroral evidence of a localized magnetic anomaly in Jupiter's northern hemisphere. *Journal of Geophysical Research*, *113*(A9), A09201. <https://doi.org/10.1029/2008JA013185>
- Grodent, D., Clarke, J. T., Waite, J. H., Cowley, S. W. H., Gérard, J.-C., & Kim, J. (2003). Jupiter's polar auroral emissions. *Journal of Geophysical Research*, *108*(A10), 1366. <https://doi.org/10.1029/2003JA010017>
- Gustin, J., Gérard, J. C., Grodent, D., Gladstone, G. R., Clarke, J. T., Pryor, W. R., et al. (2013). Effects of methane on giant planet's UV emissions and implications for the auroral characteristics. *Journal of Molecular Spectroscopy*, *291*, 108–117. <https://doi.org/10.1016/j.jms.2013.03.010>
- Hue, V., Gladstone, G. R., Greathouse, T. K., Kammer, J. A., Davis, M. W., Bonfond, B., et al. (2019). In-flight Characterization and Calibration of the Juno-ultraviolet Spectrograph (Juno-UVS). *The Astronomical Journal*, *157*(2), 90. <https://doi.org/10.3847/1538-3881/aafb36>
- Jackman, C. M., Knigge, C., Altamirano, D., Gladstone, G. R., Dunn, W., Elsner, R., et al. (2018). Assessing Quasi-Periodicities in Jovian X-Ray Emissions: Techniques and Heritage Survey. *Journal of Geophysical Research: Space Physics*, *123*(11), 9204–9221. <https://doi.org/10.1029/2018JA025490>
- MacDowall, R. J., Kaiser, M. L., Desch, M. D., Farrell, W. M., Hess, R. A., & Stone, R. G. (1993). Quasiperiodic Jovian Radio bursts: Observations from the Ulysses Radio and Plasma Wave Experiment. *Planetary and Space Science*, *41*(11), 1059–1072. [https://doi.org/10.1016/0032-0633\(93\)90109-F](https://doi.org/10.1016/0032-0633(93)90109-F)
- Manners, H., Masters, A., & Yates, J. N. (2018). Standing Alfvén Waves in Jupiter's Magnetosphere as a Source of 10- to 60-Min Quasiperiodic Pulsations. *Geophysical Research Letters*, *45*(17), 8746–8754. <https://doi.org/10.1029/2018GL078891>
- Mauk, B. H., Clarke, J. T., Grodent, D., Waite, J. H., Paranicas, C. P., & Williams, D. J. (2002). Transient aurora on Jupiter from injections of magnetospheric electrons. *Nature*, *415*, 1003–1005. <https://doi.org/10.1038/4151003a>
- McKibben, R. B., Simpson, J. A., & Zhang, M. (1993). Impulsive bursts of relativistic electrons discovered during Ulysses' traversal of Jupiter's dusk-side magnetosphere. *Planetary and Space Science*, *41*, 1041–1058. [https://doi.org/10.1016/0032-0633\(93\)90108-E](https://doi.org/10.1016/0032-0633(93)90108-E)
- Nichols, J. D., Badman, S. V., Bagenal, F., Bolton, S. J., Bonfond, B., Bunce, E. J., et al. (2017a). Response of Jupiter's auroras to conditions in the interplanetary medium as measured by the Hubble Space Telescope and Juno. *Geophysical Research Letters*, *44*(15), 7643–7652. <https://doi.org/10.1002/2017GL073029>

- Nichols, J. D., Clarke, J. T., Gérard, J. C., & Grodent, D. (2009). Observations of Jovian polar auroral filaments. *Geophysical Research Letters*, 36, 8101. <https://doi.org/10.1029/2009GL037578>
- Nichols, J. D., Yeoman, T. K., Bunce, E. J., Chowdhury, M. N., Cowley, S. W. H., & Robinson, T. R. (2017b). Periodic emission within Jupiter's Main Auroral Oval. *Geophysical Research Letters*, 44(18), 9192–9198. <https://doi.org/10.1002/2017GL074824>
- Pallier, L., & Prangé, R. (2001). More about the structure of the high latitude Jovian aurorae. *Planetary and Space Science*, 49(10), 1159–1173. [https://doi.org/10.1016/S0032-0633\(01\)00023-X](https://doi.org/10.1016/S0032-0633(01)00023-X)
- Pallier, L., & Prangé, R. (2004). Detection of the southern counterpart of the Jovian northern polar cusp: Shared properties. *Geophysical Research Letters*, 31(6), L06701. <https://doi.org/10.1029/2003GL018041>
- Pryor, W. R., Stewart, A. I. F., Esposito, L. W., McClintock, W. E., Colwell, J. E., Jouchoux, A. J., et al. (2005). Cassini UVIS observations of Jupiter's auroral variability. *Icarus*, 178(2), 312–326. <https://doi.org/10.1016/j.icarus.2005.05.021>
- Swithenbank-Harris, B. G., Nichols, J. D., & Bunce, E. J. (2019). Jupiter's Dark Polar Region as Observed by the Hubble Space Telescope During the Juno Approach Phase. *Journal of Geophysical Research: Space Physics*, 124(11), 9094–9105. <https://doi.org/10.1029/2019JA027306>
- Vogt, M. F., Bunce, E. J., Kivelson, M. G., Khurana, K. K., Walker, R. J., Radioti, A., et al. (2015). Magnetosphere-ionosphere mapping at Jupiter: Quantifying the effects of using different internal field models. *Journal of Geophysical Research: Space Physics*, 120(4), 2584–2599. <https://doi.org/10.1002/2014JA020729>
- Vogt, M. F., Kivelson, M. G., Khurana, K. K., Walker, R. J., Bonfond, B., Grodent, D., et al. (2011). Improved mapping of Jupiter's auroral features to magnetospheric sources. *Journal of Geophysical Research*, 116(A3), A03220. <https://doi.org/10.1029/2010JA016148>
- Waite, J. H., Gladstone, G. R., Lewis, W. S., Goldstein, R., McComas, D. J., Riley, P., et al. (2001). An auroral flare at Jupiter. *Nature*, 410, 787–789. <https://doi.org/10.1038/35071018>
- Weigt, D. M., Jackman, C. M., Dunn, W. R., Gladstone, G. R., Vogt, M. F., Wibisono, A. D., et al. (2020). Chandra Observations of Jupiter's X-ray Auroral Emission During Juno Apojove 2017. *Journal of Geophysical Research: Planets*, 125(4), e2019JE006262. <https://doi.org/10.1029/2019JE006262>
- Wibisono, A. D., Branduardi-Raymont, G., Dunn, W. R., Coates, A. J., Weigt, D. M., Jackman, C. M., et al. (2020). Temporal and spectral studies by XMM-Newton of Jupiter's X-ray auroras during a compression event. *Journal of Geophysical Research: Space Physics*, 125(5), e2019JA027676. <https://doi.org/10.1029/2019JA027676>
- Zhang, B., Delamere, P. A., Yao, Z., Bonfond, B., Lin, D., Sorathia, K. A., et al. (2020). *How Jupiter's unusual magnetospheric topology structures its aurora*. e-prints arXiv:2006.14834.